ACS APPLIED MATERIALS & INTERFACES

Research Article

www.acsami.org

Blister Packing of Copper Hydroxide and Titania Nanoparticles on Graphene and Its Recycling

Vadahanambi Sridhar, Deepa Gangaraju, Ho-Hwan Chun, and Hyun Park*

Global Core Research Center for Ships and Offshore Plants (GCRC-SOP), Pusan National University, Busan 609-735, Republic of Korea

ABSTRACT: Metal nanoparticles anchored on a graphene substrate find many applications such as sensors, catalysts, lithium ion batteries, etc. However, to date, graphene−metal nanohybrids have been synthesized by either covalent or ionic interactions between the graphene substrate and the metal nanoparticles. In this manuscript, we report a green and facile method to "bubble pack" metal nanoparticles on a graphene substrate by a simple process utilizing eco-friendly ionic liquids in conjunction with microwave heating. Copper nanoparticles bubble packed on graphene showed enhanced glucose sensing when compared to covalently bonded copper/graphene hybrids. Titania nanoparticles bubble packed on graphene when applied as anode materials in lithium ion batteries exhibited two times more lithium ion retention when compared to covalently bonded titania/graphene hybrids. "End of life" disposal of nanomaterials into the environment is a growing area of concern in recent days. One way of dealing with this problem is to extend the life cycle of nanomaterials by reusing the nanomaterials in multiple applications. In this report, we also show the recyclability of our novel bubble packaging material, by etching out the metal nanoparticles resulting in a unique 3D hierarchical graphene nanocup decorated graphene. The applicability of this recycled material in super capacitors is also reported.

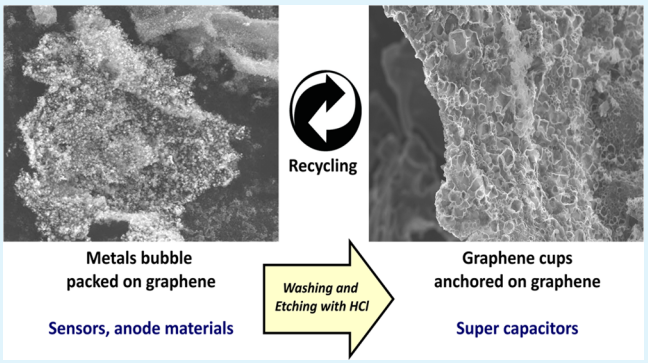

KEYWORDS: *graphene, 3D nanostructures, sensors, recycling, lithium ion battery, super capacitors*

INTRODUCTION

Graphene, an atomically thin 2-D aromatic sheet of hexagonal sp^2-bonded carbon atoms with exceptionally high mechanical stiffness, electrical transport, and thermal conductivity, is a promising material in super capacitors,[1] sensors,[2] actuators,[3] transistors,[4] hydrogels,[5] and reinforcing agents for polymers,[6] etc. Graphene possesses excellent surface area with its reported theoretical value of ∼2600 m^2/g, and this property is often utilized in hybridizing graphene with a wide range of materials like metals,[7] carbon nanotubes,[8] polymers, etc. Of these graphene hybrids, metal decorated graphene is extensively studied and finds many applications such as sensors,[9] catalysts,[10] in water purification,[11] lithium ion batteries,[12] etc. In general, the synthesis of metal−graphene hybrids, either graphene or metal nanoparticles or both, is covalently functionalized to "anchor" the metal particles on graphene substrates. Although this functionalization helps in anchoring the metal nanoparticles on a graphene substrate, it often leads to decreased catalytic activity of the metals due to the covalent "interface" layer which partially blocks the activity of the metal nanoparticles. Though there are some reports[13] on the "self assembly" of metals on graphene, they usually involve anionic surfactants like SDS (sodium 1-dodecanesulfonate) or polyethylene glycol based Triton surfactants, and in these surfactant-based systems, the anchoring mechanism of metal nanoparticles on the graphene substrate is still dependent on the formation of micelles. Therefore, there is a need for developing a technique to physically pack and anchor metal nanoparticles on the graphene substrate.

Blister packaging or bubble pack, pioneered by pharmaceutical industries, is a form−fill−seal packaging process with a thermo-formable substrate (mostly alumina or paperboard) and polyethylene terephthalate (PET) as the covering material, and this technique is fast catching up as a tamper-proof packaging technique in OTC (over the counter) and small electronic goods. Taking inspiration from this, we report a fast and facile technique to "blister pack" metal nanoparticles on a graphene substrate by using ionic liquids as the carbon source. Ionic liquids due to their intrinsic nonvolatile nature are very stable until the onset of the decomposition process and can act as a rich source of carbon. On the basis of this theory, carbonization of poly(ionic liquids) in the presence of different metallic salts has yielded an array of graphitic nanostructures such as graphene nanosheets,[14] nanotubes,[15] nanocups,[16] and nanobubbles.[17] We report a fast and facile synthesis technique to blister pack copper hydroxide and titania nanoparticles on the graphene substrate. The utility of blister-packed copper hydroxide/graphene ($Cu(OH)_2$-bp-G) in glucose sensing and

Received: July 4, 2013
Accepted: November 20, 2013
Published: November 20, 2013

titania/graphene (TiO_2-bp-G) as anode materials in lithium ion batteries is reported. Disposal of engineered nanomaterials into the environment is a serious issue. There are growing concerns about the "end of life" disposal of carbonaceous nanomaterials like CNTs, fullerene, and graphene. One way of dealing with this problem is to extend the life cycle of nanomaterials by reusing the nanomaterials in multiple applications. In this article, we also show the recyclability of this graphene packaging material, by etching out the metal nanoparticles with dilute hydrochloric acid resulting in a unique 3D hierarchical graphene nanocup decorated graphene. The utility of this recycled material in super capacitors is also reported.

EXPERIMENTAL SECTION

Synthesis of Graphene Oxide. Graphene oxide was prepared by the modified Hummers methods. Briefly, 1 g of graphite and 0.5 g of $NaNO_3$ were placed in a 250 mL round-bottom flask, and then 25 mL of H_2SO_4 was poured drop-wise under constant stirring in an ice-bath. Subsequently, 3 g of $KMnO_4$ was added into the reaction system. The system was allowed to reach room temperature, 32 °C, and maintained for 30 min. Next, 50 mL of deionized water was slowly added into the flask, and then the temperature of this mixture was slowly increased to 98 °C and kept for 15 min. Afterwards, 80 mL of deionized water was added to dilute the viscous mixture, followed by addition of 30 % H_2O_2 to remove remnants of $KMnO_4$ until the solution turned golden yellow. Then the mixture was centrifuged at 12 000 rpm for 5 min. The sediments were washed with deionized water until the pH value of supernatant liquor of the suspension was close to 7. The sediment was redispersed in deionized water, ultrasonicated, and filtered, and finally the filter cake was dried in vacuum at 70 °C for 24 h.

Synthesis of Metal Nanoparticles Blister-Packed on Graphene. Our simple procedure for blister packing metal nanoparticles on graphene involves these reagents: graphene oxide; the metal nanoparticle precursors, titanium di-isopropoxide bis(acetylacetonate) or copper acetyl acetonate catalytic precursor; and the carbon source, 1-ethyl-3-methylimidazolium tetrafluoroborate (EMIM BF_4). These precursors are mixed in a weight ratio of 2:0.2:0.5 in iso-propanol solvent and subjected to ultrasonication for 60 min. Subsequently, the mixture was irradiated for 5 min in a microwave oven operating at 700 W yielding a fluffy powdered product.

Material Characterization. The synthesized nanomaterials were characterized by field-emission scanning electron microscopy (FE-SEM, Nova NanoSEM 230 FEI operating at 15 kV), transmission electron microscopy (JEM-3011HR microscope operating at 200 kV), X-ray diffraction (XRD, Rigaku D/max-2550 V, Cu-Ka radiation), Raman spectra (LabRAM HR UV/vis/NIR Horiba Jobin-Yvon, France), and X-ray photoelectron spectroscopy (Sigma Probe Thermo VG spectrometer using Mg Kα X-ray sources). The XPS spectra were curve fitted with a mixed Gaussian−Lorentzian shape using the freeware XPSPEAK.

Electrode Preparation for Glucose Sensing. The glassy carbon electrode was successively polished with 1.0, 0.3, and 0.05 μm alumina slurry and sonicated in 1:1 nitric acid, absolute alcohol, and double-distilled water. The cleaned electrode was dried in a stream of high-purity nitrogen. A $Cu(OH)_2$-bp-G nanocomposite modified glassy carbon electrode (GCE) was prepared by casting 5 μL of $Cu(OH)_2$-bp-G suspension (10 mL of *N*,*N*-dimethylformamide (DMF)) on the GCE surface and dried.

Anode Performance and Super-Capacitor Test. Electrochemical tests were conducted using CR2032 coin-type test cells assembled in an argon-filled glovebox. The working electrodes were composed of approximately 0.3−0.6 mg of active material and a lithium foil separated by a microporous Celgard 2400 membrane. The electrolyte solution was prepared by dissolving 1 M $LiPF_6$ in a 1:1 mass ratio mixture of ethylene carbonate and dimethyl carbonate. Galvanostatic charge−discharge cycling tests were performed using an WBCS 3000, Won-A-Tech, Kore,a battery testing system in the voltage range between 0 and 3 V. The super-capacitor tests of 3D Gcup@G hybrid materials were carried out based on the protocol reported in our earlier publication.[15]

RESULTS AND DISCUSSION

The overall synthesis procedure of bubble packing metal nanoparticles on a graphene substrate is shown schematically in Figure 1. As a test case, two metals, namely, copper and

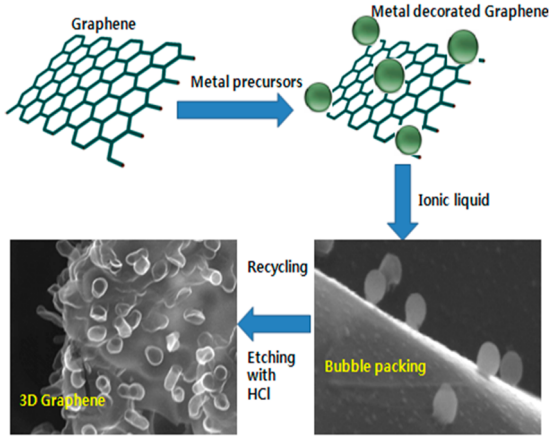

Figure 1. Schematic diagram of synthesis and recycling of bubble packed graphene.

titanium, were bubble packed on the graphene substrate, and the synthesis procedure is simple, based on our previously reported ionic liquid based synthesis of graphene/carbon nanotube hybrids.[15,16]

The mechanism of bubble packing of metal nanoparticles on a graphene substrate can be explained as follows: in the ultrasonication step, the 1-ethyl-3-methylimidazolium tetrafluoroborate intercalates into the interstatial gaps of graphite oxide sheets and results in its partial exfoliation.[18] During the initial stages of microwave irradiation, the metal precursor, copper acetylacetonate, is coordinately dissolved by the BF_4^- anion and forms copper nanoparticles. These nanoparticles are attached on the graphene substrate by anchoring onto the defects generated on the graphene sheet by microwave irradiation of the graphene sheet. Subsequently, when this mixture is subjected to microwave irradiation, the graphite oxide platelets are rapidly exfoliated[15] (accompanied by sparkling and a cracking sound) to form graphene nanosheets. With further irradiation, the imidazolium moiety of the ionic liquid decomposes to produce carbonaceous gases, which are captured by the metal nanoparticles to form bubble packed copper nanoparticles pinned onto the graphene substrate ($Cu(OH)_2$-bp-G).

The morphology and microstructure of copper nanoparticles blister packed on graphene were examined by scanning electron microscopy (SEM) and high-resolution transmission electron microscopy (HR-TEM). Figure 2(a) shows well-dispersed and distributed copper nanoparticles on the graphene sheet with minimal agglomeration and relatively high concentration of the nanoparticles on the graphene substrate. This dispersion and distribution of copper without any considerable aggregation is also reflected in TEM micrographs in Figure 2(b) wherein spherical copper nanoparticles encapsulated in multishelled graphene coating (indicated by arrows in the figure) with a relatively low degree of polydispersion in particle size distribution is observed. In the absence of surfactants, it is

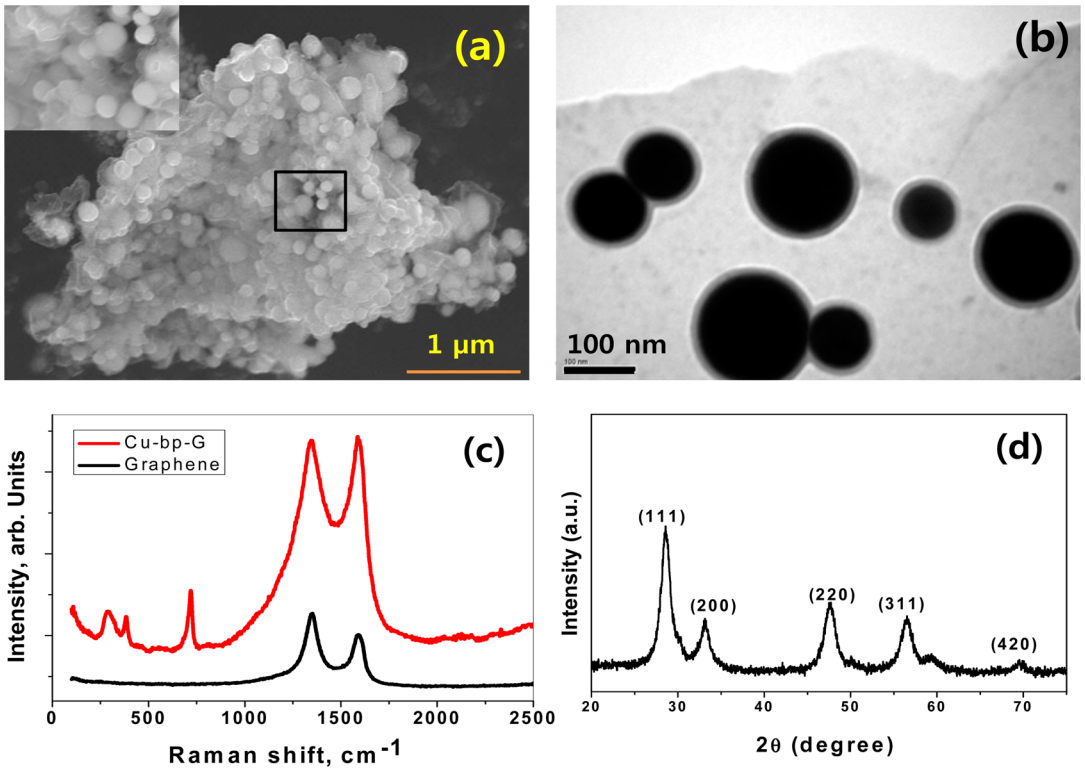

Figure 2. SEM (a), TEM (b), Raman spectra (c), and XRD spectra (d) of copper nanoparticles bubble packed on graphene.

generally known that sol−gel-derived nanoparticles show a high degree of aggregation and agglomeration when compared to synthesis methods like CVD, atomic layer deposition, or electrochemical techniques. To minimize this aggregation, surfactants or organic capping agents are generally used. In our test case system of copper bubble packed on graphene, a relatively lower degree of agglomeration has been observed which can be explained based on two phenomena: first is anchoring of nanoparticles on the defect sites of graphene induced by microwave radiation, and second is the formation of a graphene protective layer around the nanoparticles which stops aggregation due to Ostwald ripening.

The obtained $Cu(OH)_2$-bp-G was then tested by Raman spectra at a laser excitation frequency of 514 nm excitation (Figure 2(c)). In the case of Cu-b-G three-dimensional (3-D) materials, there are five peaks in the range of 1000−4000 cm^{-1}. The peak at 1586 cm^{-1} is the Raman active G band originating from the in-plane vibrational mode, and the peak at 1344 cm^{-1} is due to disorder-induced in-plane substitutions and defects. In the region of the lower-order Raman spectrum, three peaks are attributed to the presence of copper nanoparticles at 290.5, 384.1, and 718.3 eV. The I_D/I_G ratio (ratio of intensities of D and G bands) is a valuable tool to qualitatively assess the degree of ordering in carbon nanostructures. The I_D/I_G ratio of $Cu(OH)_2$-bp-G nanostructures exhibits a lower value of 0.98 when compared to that of graphene (1.19), implying that there is a partial healing of defects due to anchoring of copper nanoparticles.[19]

The crystallinity and chemical composition of $Cu(OH)_2$-bp-G were investigated by X-ray diffraction (XRD) and X-ray photoelectron spectroscopy (XPS), respectively. The XRD pattern of Cu-bp-G is plotted in Figure 2(d). The strong diffraction peaks at 28.6, 33.3, 47.7, 56.44, and 69.4° are in good agreement with (111), (200), (220), (311), and (420) crystal planes of copper hydroxide ($Cu(OH)_2$), albeit there is a blue shift of about 1−2° observed in all the peaks. This shift can be attributed to the interference due to the graphene coating on the copper nanoparticles. Assuming that $Cu(OH)_2$ particles are spherical, the average copper metal crystallite sizes were calculated from the full width at half-maximum (fwhm) of the diffraction lines. The calculated results show that the average particle size is in the range of 38−160 nm, and the calculated values are in line with the diameters of nanoparticles observed in the TEM image.

XPS spectra of the Cu(2p) binding energy region plotted in Figure 3(a) show two main peaks at 934.7 and 954.7 eV corresponding to $Cu(2p_{3/2})$ and $Cu(2p_{1/2})$, respectively, in addition to a small shake up signal at 944.9 eV. The ratio of the areas of the two peaks, $A_{(Cu\ 2p3/2)}/A_{(Cu\ 2p1/2)}$, is equal to 3.1, and the binding energy (BE) difference, $E_{b(Cu\ 2p1/2)} - E_{b(Cu\ 2p3/2)}$, is 20 eV. These observed values indicate that Cu exists in the Cu^{2+} state in the form of $Cu(OH)_2$ on the surface. There are some reports[20] which attribute the formation of 934.7 eV to malachite, $Cu_2(CO_3)(OH)_2$. The deconvoluted XPS analysis of the C(1s) core level spectrum shown in Figure 3(b) exhibits a predominant peak at 284.5 eV attributed to the C−C, C═C, and C−H bonds, and the weak deconvoluted peak centered at 281.8 eV is assigned to carbon-coated copper nanoparticles. The other minor peaks at 286.2, 287.6, and 288.8 eV are assigned to the C−OH, C═O, and O═C−OH functional groups, respectively. XPS and XRD analysis confirms that graphene-coated cuprous hydroxide nanoparticles are formed by our microwave technique.

The utility of $Cu(OH)_2$-bp-G in electrochemical hydrogen peroxide sensing was investigated. Sensing and monitoring of H_2O_2 is very critical in clinical, food, environmental, pharmaceutical, and many biological reactions, especially in monitoring of diabetes, since H_2O_2 is liberated in the enzymatic

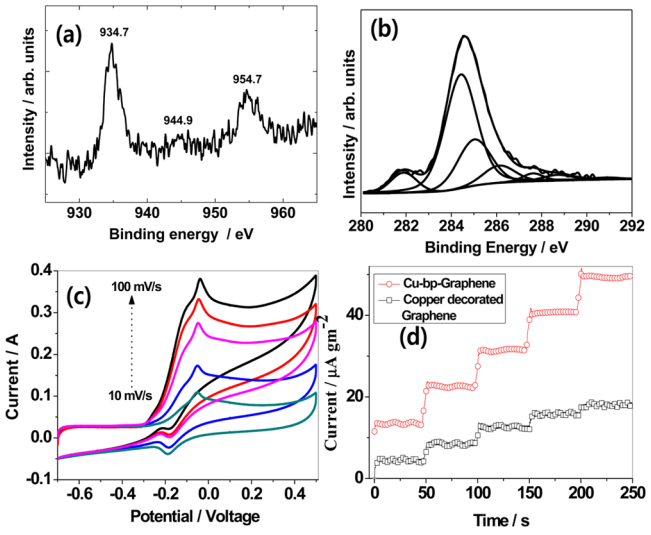

Figure 3. Cu 3p (a) and deconvoluted C 1s (b) XPS spectra of copper blister packed on graphene. Cyclic voltammograms of $Cu(OH)_2$-bp-G in 1.0 mM H_2O_2 in 0.1 M NaOH solution at a scan rate of 10−100 mV s^{-1}(c). Transient response of $Cu(OH)_2$-bp-G and copper decorated graphene to glucose (d).

reaction. Enzymeless nanoparticle-based electrochemical monitoring is gaining attention in recent days. Of all the metals investigated, copper nanoparticles are most efficient due to their high selectivity and fast response. However, copper has a tendency to oxidize quickly resulting in a progressive decrease in sensing. So, graphene-protected copper nanoparticles anchored onto a conductive substrate like graphene can be very useful. Figure 3(c) shows the cyclic voltammograms of $Cu(OH)_2$-bp-G in 1.0 mM H_2O_2 in 0.1 M NaOH solution. One anodic peak corresponding to oxidation of $Cu(OH)_2$ and one reduction peak can be observed. This is contrary to the usual three anodic and two cathodic peaks normally observed in copper decorated graphene.[21] Figure 3(d) shows the amperometric transient response of graphene and $Cu(OH)_2$-bp-G electrodes at successive additions of 50 μM glucose injected into 0.1 M NaOH electrolyte solution at intervals of 50 s. In the case of copper decorated graphene modified electrodes, the response progressively gets weaker after two to three spikes, whereas in the case of $Cu(OH)_2$-bp-G the response is constant. This shows that the graphene shells on the copper nanoparticles act as effective shields protecting the oxidation of copper and keeping intact its sensing capability.

Titania nanoparticles bubble packed on graphene were also synthesized by a similar procedure and morphology of the nanocomposites tested by SEM and TEM. The representative SEM micrograph shown in Figure 4(a) shows uniformly distributed and well-dispersed core-shelled titania nanoparticles anchored onto the graphene sheet, whereas the high-resolution TEM image (Figure 4(b)) exhibits titania nanoparticles of 10−30 nm diameters embedded in a graphene shell. Recently, titania anchored on graphene has attracted attention as anode material for lithium ion batteries. When compared to other metals like iron, cobalt, and nickel, titania offers advantages such as high lithium insertion and extraction and less formation of solid electrolyte interface layers which improves the safety and life cycle of the batteries. However, the main disadvantage

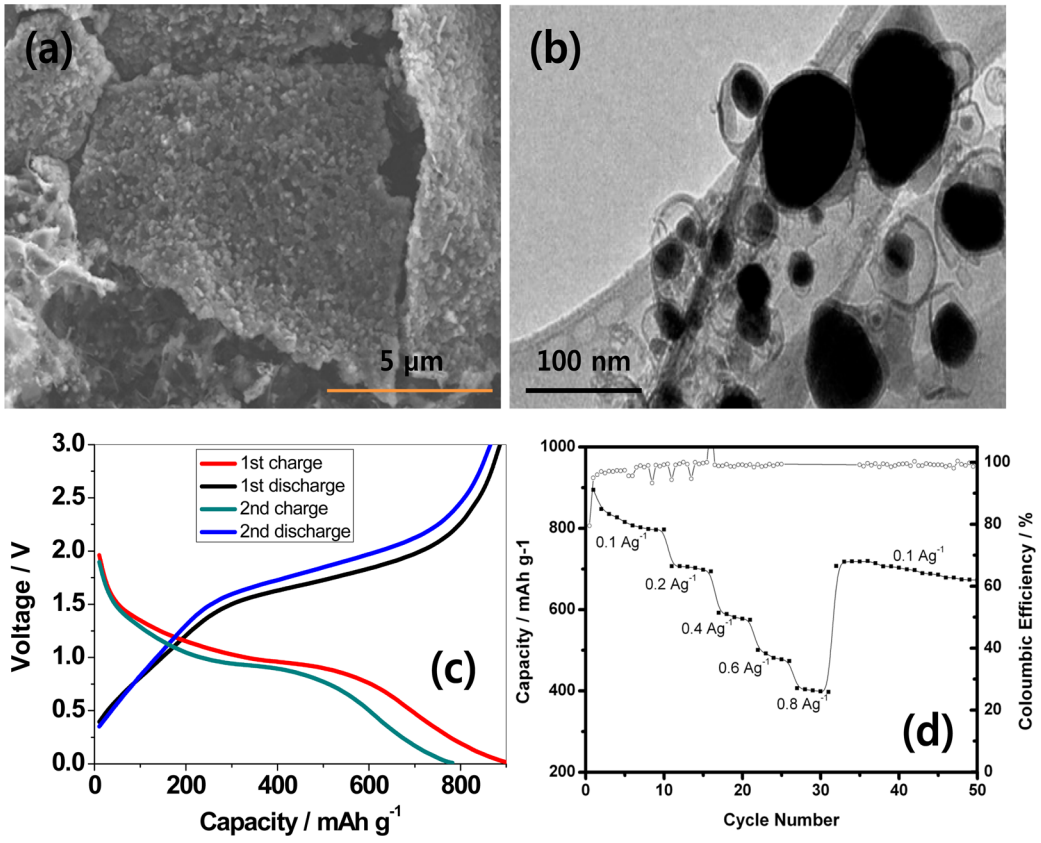

Figure 4. SEM (a) and high-resolution TEM (b) micrographs of titania bubble packed on graphene. First and second cycles of galvanostatic charge/discharge curves of TiO_2-bp-G (c). Cyclic performance and Coloumbic efficiency at different current densities (d).

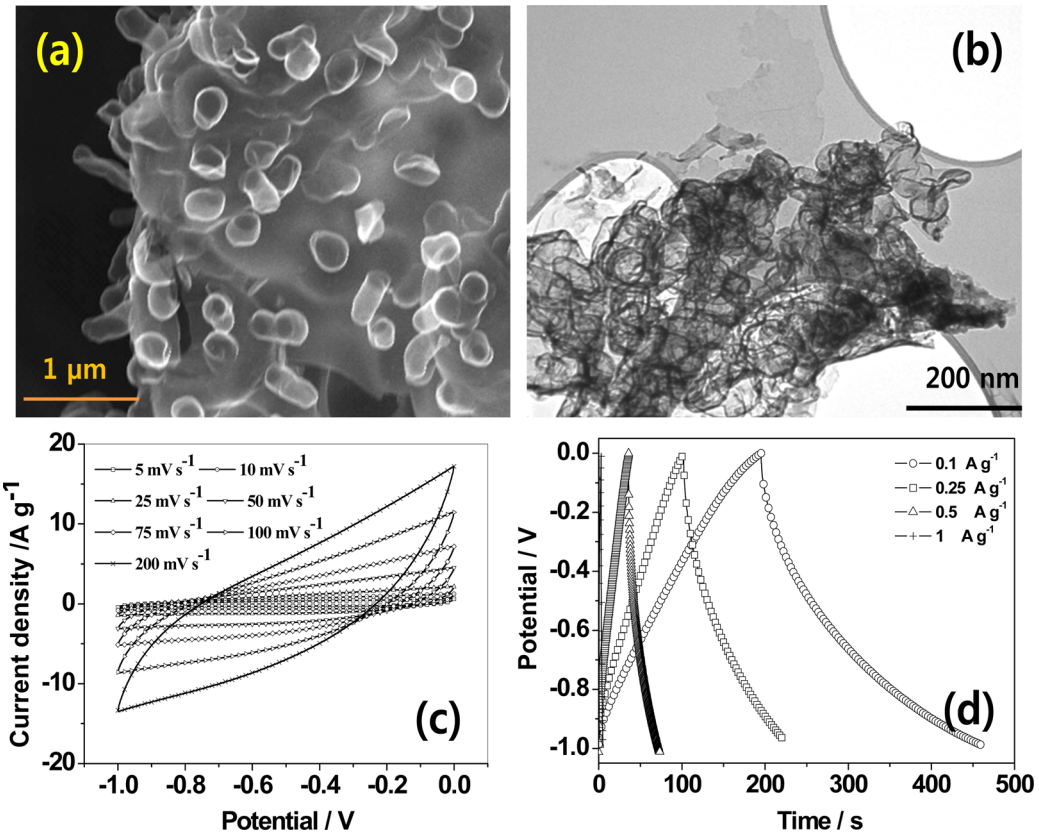

Figure 5. SEM (a) and high-resolution TEM micrographs (b) of graphene cups anchored on graphene 3D nanostructures after recycling and acid etching of Cu-bp-G; CV curves of supercapacitors based on Gcup@G nanostructures at different scan rates (c). Charge/discharge curves at different current densities (d).

of titania is its very low conductivity which limits its electrochemical performance. In this aspect, titania bubble packed on graphene (TiO_2-bp-G) can be very useful in increasing the conductivity of titania. The electrochemical performance of TiO_2-bp-G was evaluated in lithium half cells, and the charge−discharge behavior of the first two cycles is shown in Figure 3(c) at a scan rate of 0.1 C within a cutoff window of 1.0−3.0 V. The discharge and charge capacities are more than five times higher than the theoretical capacity of titania (167.5 mAh g^{-1}) and more than double the reported values in titania decorated graphene.[22,23] This outstanding electrochemical performance can be attributed to the unique blister packing of nanosized titania on the graphene substrate. Two synergistic phenomena, anchoring and distribution of nanosized titania on a graphene substrate that results in shorter Li^+ diffusion path lengths and its subsequent packing of these nanoparticles by graphene, prevent the agglomeration of nanoparticles, ensure good electronic conductivity, mitigate the large volume changes occurring during lithiation reaction, and contribute to enhanced electrochemical performance.[24,25] The shapes of the charge−discharge curve provide valuable information about the storage of lithium ions. Unlike in conventional titania decorated graphene that shows a flat charge and discharge voltage plateau at 1.98 and 1.7 V, respectively, in our system of TiO_2-bp-G, the typical "marching" slope-like charge−discharge curves with no plateau phenomenon are observed. This is typical capacitive behavior of the surface and interfacial storage of lithium ions whose degree increases with increasing surface area. Figure 4(d) shows the rate capability of anode material cyclically tested from 1 to 8 C at five charge/discharge cycles at each rate. Even at high rates of 8 C, our system of TiO_2-bp-G delivered a favorable capacity of ∼420 mAhg. When the current rate was returned to 0.1 C, the stable high capacity of 725 mAhg was resumed.

Given the increasing production and utility of nanomaterials in many applications, the danger of its release into the environment and into the ecosystem is a major concern these days. One way to deal with this problem is recycling of nanomaterials in multiple applications. In this work, we also demonstrate a proof-of-concept of recycling of our blister packed nanomaterials. The $Cu(OH)_2$-bp-G nanoparticles after testing as a glucose sensor were recovered and repeatedly washed with deionized water and dilute hydrochloric acid to extract out all the copper nanoparticles. The morphology of the so-obtained product resulted in a unique morphology of graphene nanocups anchored onto the graphene substrate (Gcup@G).

Representative SEM and TEM micrographs of the Gcup@G are shown in Figures 5(a) and 5(b), respectively. Well-dispersed nanometer-sized graphene cups all along the surface of the graphene sheet can be observed from the SEM image. The TEM micrographs show that the cups of graphene are open and hollow with an average wall thickness of ∼6 to ∼8 nm, and this free space of the bowls can be very advantageous in a variety of applications especially in super capacitors. Recently, much attention has been focused on the utility of mesoporous graphene in super-capacitor applications. This mesoporous architecture leads to significant enhancement in surface areas which will be very helpful in energy applications like electric double-layer capacitors (EDLCs). However,

generally the mesoporous structure in graphene is obtained either by destructive techniques like KOH activation or plasma bombardment to induce disorder and defects on its surface. However, the presence of substantial defects on the graphene surface is detrimental to the structural health of graphene sheets. One way to overcome this problem is by adding mesoporous graphene structures onto the graphene substrate, and our technique is one simple way of doing this. Figure 5(c) presents the cyclic voltammetry (CV) curves of Gcup@G electrodes tested in an aqueous electrolyte of 30 wt % KOH at scan rates of 5−100 mV within the potential window ranging from 0 to −1 V. The symmetric and nearly rectangular CV curves indicate the typical electrical double-layer capacitive behavior with very rapid current response on voltage reversal. The CV curve still remains nearly rectangular without apparent distortion even at a scan rate of 100 mV s. The specific electrode capacitance (Cg) of Gcup@G is about 307 F g (based on the mass of RGO) at a scan rate of 5 mV s. This excellent electrochemical performance can be ascribed to prevention of the aggregation of graphene nanosheets by the graphene cups which act as effective spacers. These spacers can significantly improve the accessible specific surface area and enhance the utilization of mesopores of Gcup@G electrode material. Galvanostatic charge−discharge curves of the Gcup@G at different current densities are shown in Figure 5(d). The charge−discharge curves show a nonsymmetrical behavior of voltage−time, with a slight IR drop and a sudden voltage drop (linear portion parallel to the *y*-axis) attributed to the voltage change due to the internal resistance and a capacitive component (curved convex portion) related to the voltage change due to variation in energy within the capacitor, indicating a high reversibility between charge and discharge processes. These result show that the Gcup@G have excellent capacitive performance mainly attributed to pure electric double-layer capacitance and rapid current−voltage response.

CONCLUSIONS

In summary, we developed a fast microwave technique to bubble pack metal nanoparticles on the graphene substrate. This unique architecture prevents the aggregation and agglomeration of nanoparticles without any covalent bonding. Copper nanoparticles blister packed on graphene showed higher sensing capability for glucose, whereas bubble packing titania on graphene substrate resulted in remarkable lithium ion capacity attributed to the synergistic effects of anchoring of nanosized titania on the graphene substrate and subsequent packing and sealing of these nanoparticles by a protective graphene film. Furthermore, we also showed that these blister packed nanoparticles can be recycled into the graphene nanocup anchored on the graphene substrate and can be very effective as EDLC capacitors.

AUTHOR INFORMATION

Corresponding Author

*E-mail: hyunpark@pusan.ac.kr.

Notes

The authors declare no competing financial interest.

ACKNOWLEDGMENTS

This work was supported by National Research Foundation of Korea (NRF) grant of the Korea government (MSIP) through GCRC-SOP (No. 2011-0030013) and Industrial Strategic Technology Development Program (Grant No. 10038606) funded by the Ministry of Knowledge Economy (MKE, Korea).

REFERENCES

(1) Stoller, M. D.; Park, S.; Zhu, Y.; An, J.; Ruoff, R. S. *Nano Lett.* **2008**, *8*, 3498−3502.
(2) Rumyantsev, S.; Liu, G. X.; Shur, M. S.; Potyrailo, R. A.; Balandin, A. A. *Nano Lett.* **2012**, *12*, 2294−2298.
(3) Jung, J. H.; Jeon, J. H.; Sridhar, V.; Oh, I. K. *Carbon* **2011**, *49*, 1279−1289.
(4) Li, X.; Cai, W.; An, J.; Kim, S.; Nah, J.; Yang, D.; Piner, R.; Velamakanni, A.; Jung, I.; Tutuc, E.; Banerjee, S. K.; Colombo, L.; Ruoff, R. S. *Science* **2009**, *324*, 1312.
(5) Sridhar, V.; Oh, I. K. *J. Colloid Interface Sci.* **2010**, *348*, 384−387.
(6) Li, Z.L.; Young, R. J.; Kinloch, I. A. *ACS Appl. Mater. Interfaces* **2013**, *5*, 456−463.
(7) Lin, Y.; Baggett, D. W.; Kim, J. W.; Siochi, E. J.; Connell, J. W. *ACS Appl. Mater. Interfaces* **2011**, *3*, 1652−1664.
(8) Lee, S. H.; Sridhar, V.; Jung, J. H.; Karthikeyan, K.; Lee, Y. S.; Mukherjee, R.; Koratkar, N.; Oh, I. K. *ACS Nano* **2013**, *6*, 4242−4251.
(9) Gao, H. C.; Xiao, F.; Ching, C. B.; Duan, H. W. *ACS Appl. Mater. Interfaces* **2011**, *3*, 3049−3057.
(10) Hsu, C. H.; Liao, H. Y.; Wu, Y. F.; Kuo, P. L. *ACS Appl. Mater. Interfaces* **2011**, *3*, 2169−2172.
(11) Gao, W.; Majumder, M.; Alemany, L.B.; Narayanan, T. N.; Ibarra, M. A.; Pradhan, B. K.; Ajayan, P. M. *ACS Appl. Mater. Interfaces* **2011**, *3*, 1821−1826.
(12) Qiu, J. X.; Zhang, P.; Ling, M.; Li, S.; Liu, P. R.; Zhao, H. J.; Zhang, S. Q. *ACS Appl. Mater. Interfaces* **2012**, *4*, 3636−3642.
(13) Wang, D. H.; Choi, D. W.; Li, J.; Yang, Z. G.; Nie, Z. M.; Kou, R.; Hu, D. H.; Wang, C. M.; Saraf, L. V.; Zhang, J. G.; Aksay, I. A.; Liu, J. *ACS Nano* **2009**, *3*, 907−914.
(14) Yuan, J.; Giordano, C.; Antonietti, M. *Chem. Mater.* **2010**, *22*, 5003−5012.
(15) Sridhar, V.; Kim, H. J.; Jung, J. H.; Park, S.; Oh, I. K. *ACS Nano* **2012**, *6*, 10562−10570.
(16) Sridhar, V.; Lee, I.; Yoon, H. S.; Chun, H. H.; Park, H. *Carbon* **2013**, *61*, 633−639.
(17) Soll, S.; Fellinger, T. P.; Wang, X.; Zhao, Q.; Antionetti, M.; Yuan, J. *Small* **2013**, DOI: 10.1002/smll.201300680.
(18) Lu, J.; Yang, J. X.; Wang, J. Z.; Lim, A. L.; Wang, S.; Loh, K. P. *ACS Nano* **2009**, *3*, 2367−2375.
(19) Karoui, S.; Amara, H.; Bichara, C.; Ducastelle, F. *ACS Nano* **2010**, *4*, 6114−6120.
(20) Grohmann, I.; Peplinksi, B.; Unger, W. *Surf. Interface Anal.* **1992**, *19*, 591−594.
(21) Zhang, F. Y.; Li, Y. J.; Gu, Y. E.; Wang, Z. H.; Wang, C. M. *Microchim. Acta* **2011**, *173*, 103−109.
(22) Wang, D.; Choi, D.; Li, J.; Yang, Z.; Nie, Z.; Kou, R.; Hu, D.; Wang, C.; Saraf, L. V.; Zhang, J.; Aksay, I. A.; Liu, J. *ACS Nano* **2009**, *3*, 907−914.
(23) Cao, H.; Li, B.; Zhang, J.; Lian, F.; Kong, X.; Qu, M. *J. Mater. Chem.* **2012**, *22*, 9759−9766.
(24) Zhou, J.; Song, H.; Chen, X.; Zhi, L.; Yang, S.; Huo, J.; Yang, W. *Chem. Mater.* **2009**, *21*, 2935−2940.
(25) Li, T.; Wang, Y. Y.; Tang, R.; Qi, Y. X.; Lun, N.; Bai, Y. J.; Fan, R. H. *ACS Appl. Mater. Interfaces* **2013**, *19*, 9470−9477.